Supplementary Materials

Single-Crystal Structure Analysis of Dicarboxamides: Impact of Heteroatoms on Hydrogen Bonding of Carboxamide Groups

Abdulrahman Mohabbat, Jasmin Salama, Philipp Seiffert, István Boldog and Christoph Janiak *

Institut für Anorganische Chemie und Strukturchemie, Heinrich-Heine-Universität, 40204 Düsseldorf, Germany; abdulrahman.mohabbat@uni-duesseldorf.de (A.M.); jasmin.salama@uni-duesseldorf.de (J.S.); philipp.seiffert@uni-duesseldorf.de (P.S.); boldogi@uni-duesseldorf.de (I.B.)

* *Correspondence: janiak@uni-duesseldorf.de*

Content

S1 Chemicals used.....S2

S2 Preparation of the dicarboxamides S2

S3 NMR spectra of the dicarboxamides.....S3

S4 IR spectra of the dicarboxamides S6

S5 Mass spectra of the dicarboxamides S7

S6 PXRD and Le Bail Fitting of the dicarboxamides.....S9

S7 2D Hirshfeld plots of the dicarboxamides.....S13

References S20

S1 Chemicals used

Table S1. Overview of chemicals used.

Chemical	Purity [%]	Supplier
2,5-furandicarboxylic acid	97	Sigma-Aldrich
3,5-pyridinedicarboxylic acid	>98,0	TCL
2,5-thiophenedicarboxylic acid	99,23	BLD Pharmatech Ldt.
Ammonia solution 25%	25	Merck
Deionized ultrapure water	-	Milipore
Dimethyl sulfoxide-d6	99,9	Sigma-Aldrich
Ethanol	≥99,9	ChemSolute
Methanol	≥99,9	Sigma-Aldrich
N,N-Dimethylformamide	99,5	Fisher Chemical
n-Hexane	97	VWR Chemicals
Thionyl chloride	99,7	Acros Organics

S2 Preparation of the dicarboxamides

For the synthesis of the dicarboxamides, 10 mmol of the corresponding dicarboxylic acid and 25 mL of thionyl chloride were placed in a 100 mL flask and connected to a reflux condenser. The specific amounts of each dicarboxylic acid used are listed in Table S2 . A few drops of DMF were added as a catalyst, and the mixture was heated to reflux at 90 °C overnight. The resulting solution was cooled to room temperature, and the excess thionyl chloride was removed. The remaining residue was washed three times with 15 mL of hexane and then dried under vacuum. This intermediate was then transferred to a 100 mL flask, and 5 mL of aqueous ammonia (25%) was added dropwise while stirring in an ice bath. The reaction mixture was stirred in the ice bath for one hour. After drying, the product was washed three times with 15 mL of water and ethanol, and then dried again to obtain the final product [1].

Table S2. Amount of dicarboxylic acids used for the synthesis and yield of obtained dicarboxamides.

Dicarboxylic acid	Amount [g]/[mmol]	Yield of dicarboxamides [%]
2,5-thiophenedicarboxylic acid	1.72 / 10	75
2,5-furandicarboxylic acid	1.56 / 10	62
3,5-pyridinedicarboxylic acid	1.67 / 10	60

S3 NMR spectra of the dicarboxamides

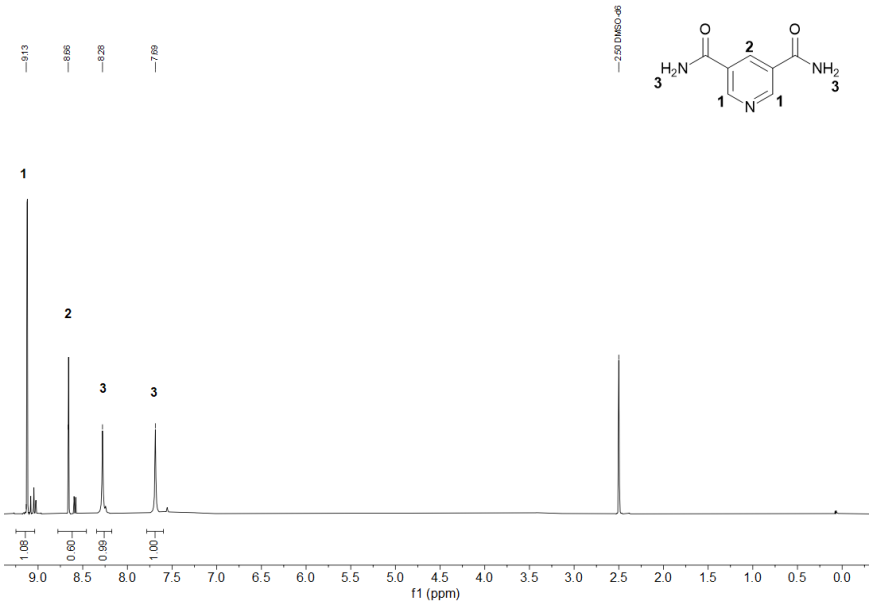


Figure S1. [1]H-NMR spectrum (600 MHz, DMSO-d$_6$) of 3,5-pyridinedicarboxamide, PDC.

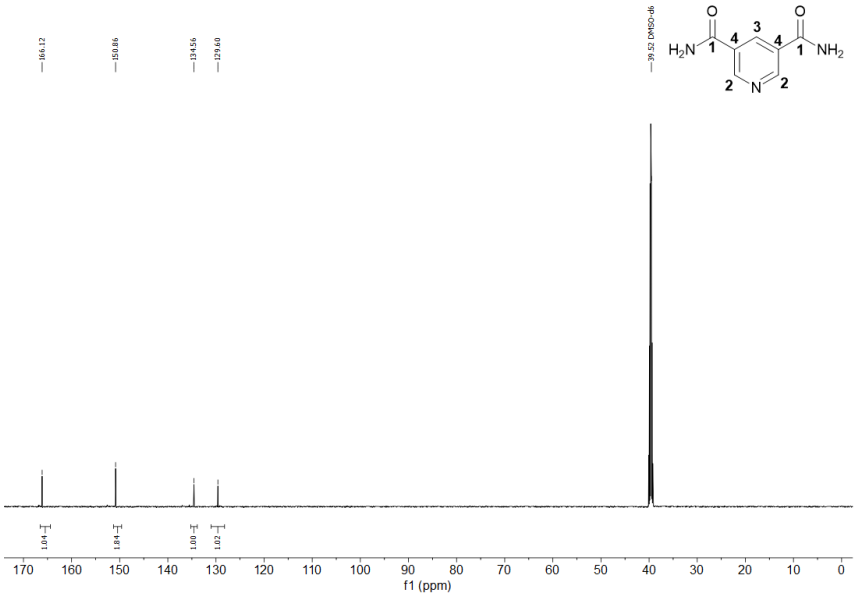


Figure S2. [13]C-NMR spectrum (75 MHz, DMSO-d6) of 3,5-pyridinedicarboxamide, PDC.

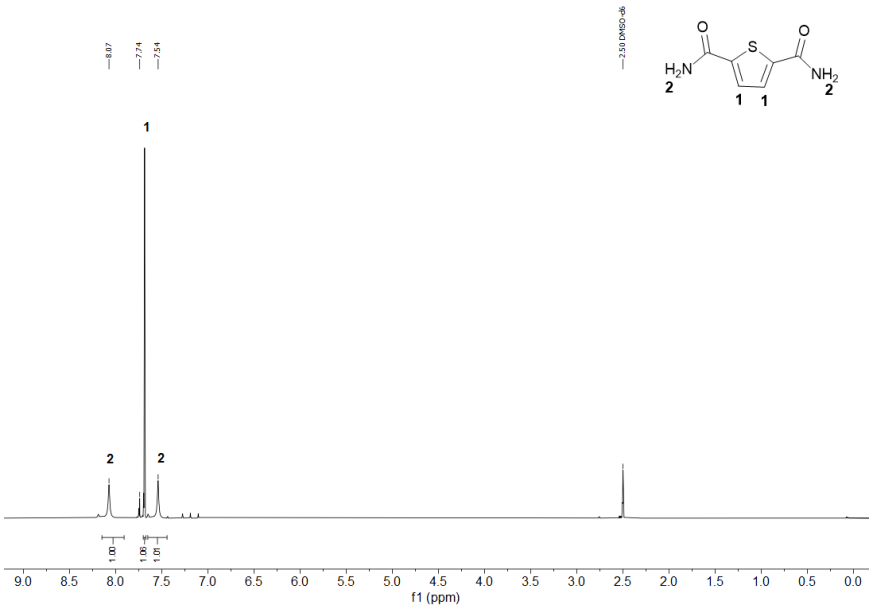


Figure S3. [1]H-NMR spectrum (600 MHz, DMSO-d6) of 2,5-thiophenedicarboxamide.TDC.

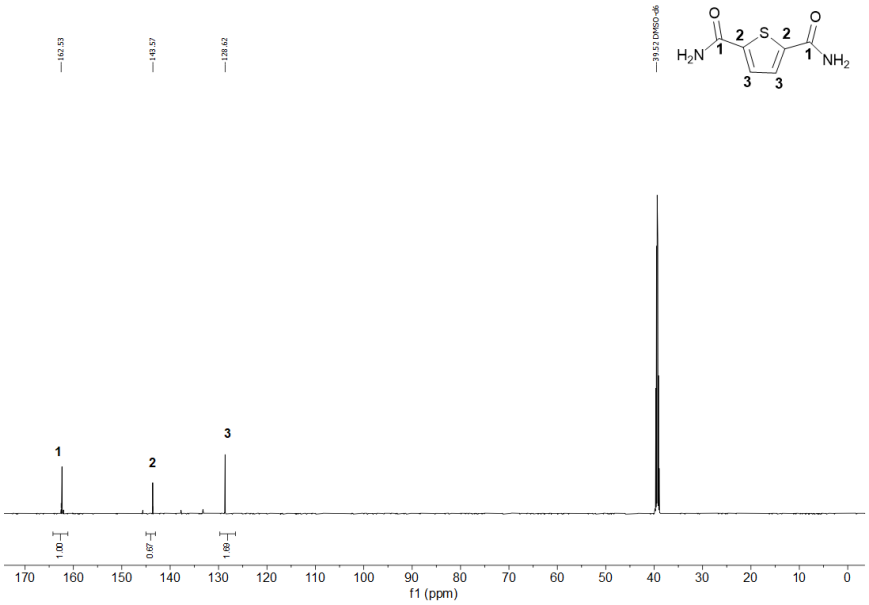


Figure S4. [13]C-NMR spectrum (75 MHz, DMSO-d_6) of 2,5-thiophenedicarboxamide, TDC.

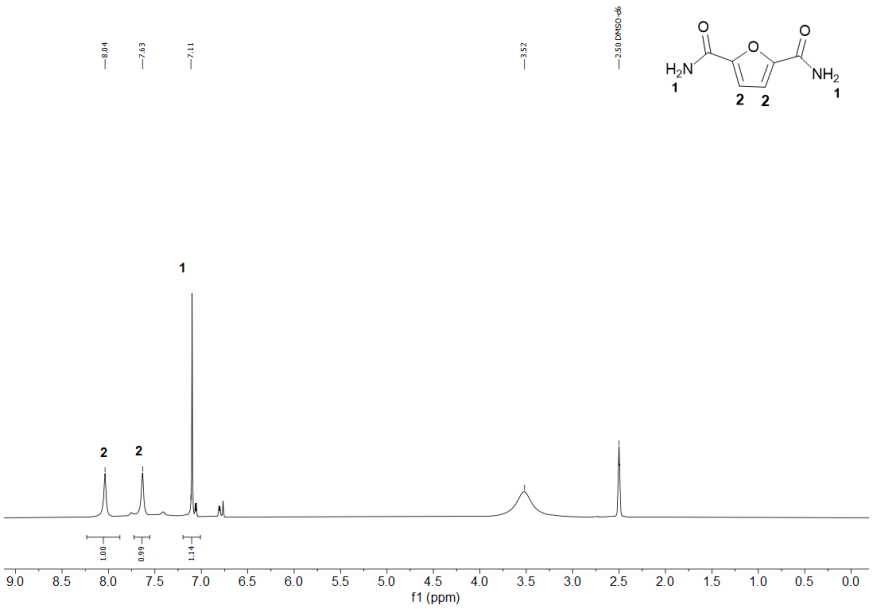


Figure S5. [1]H-NMR spectrum (600 MHz, DMSO-d6) of 2,5-furandicarboxamide, FDC.

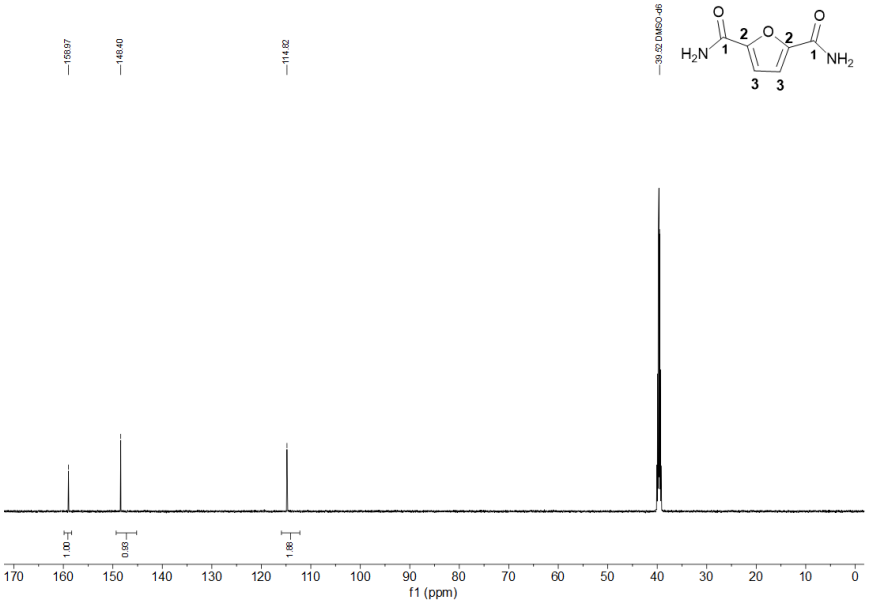


Figure S6. [13]C-NMR spectrum (75 MHz, DMSO-d6) of 2,5-furandicarboxamide, FDC.

S4 IR spectra of the dicarboxamides

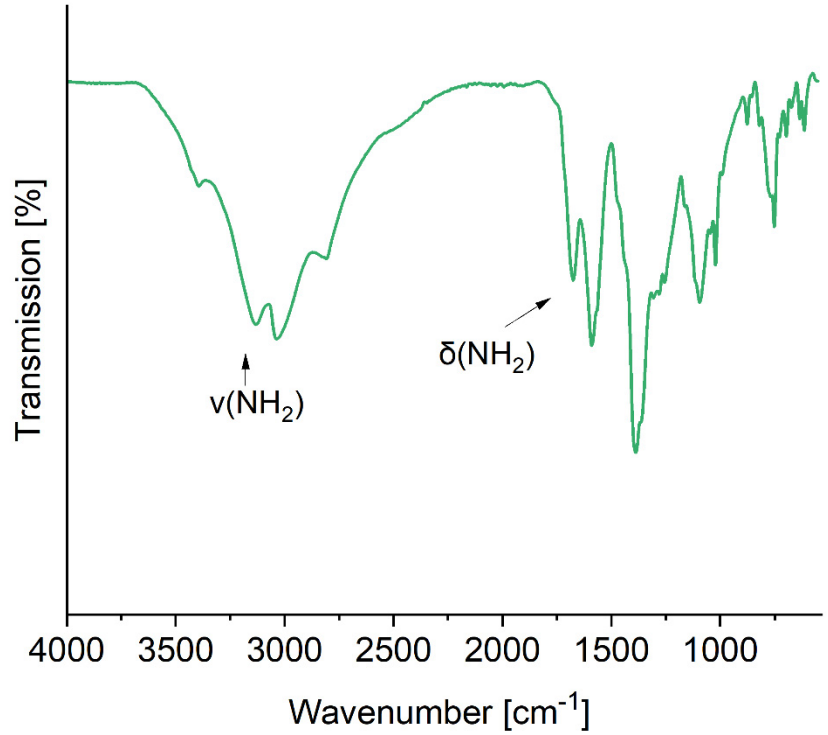


Figure S7. IR spectrum of 3,5-pyridinedicarboxamide, PDC (attenuated total reflection, ATR).

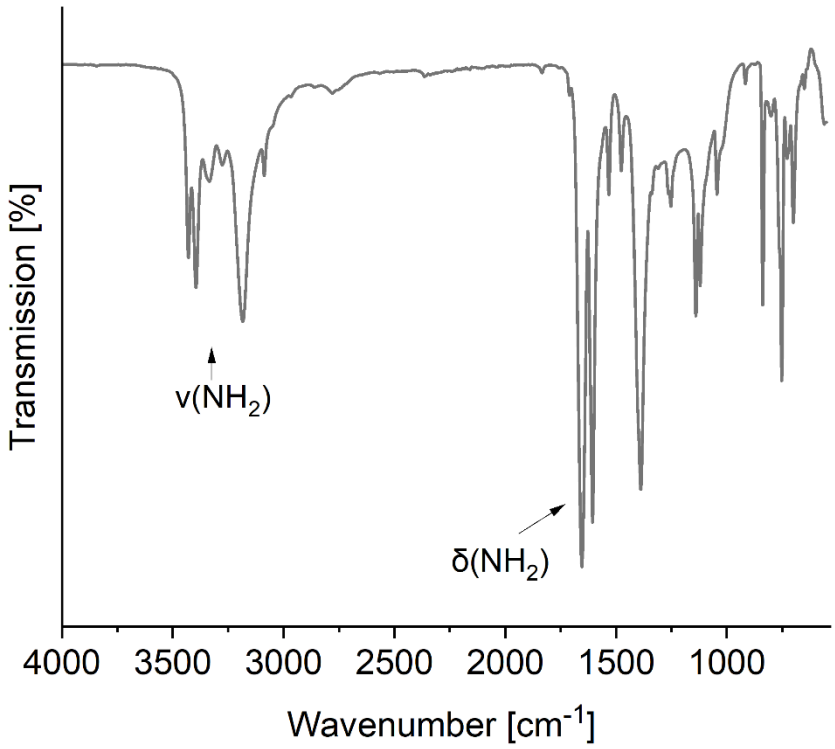


Figure S8. IR spectrum of 2,5-thiophenedicarboxamide, TDC (attenuated total reflection, ATR).

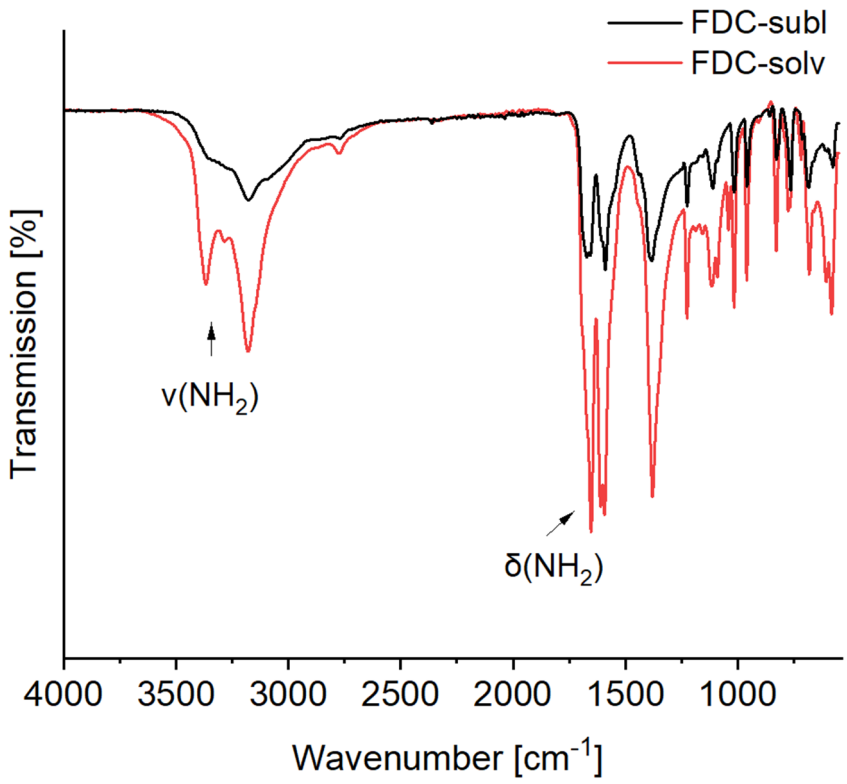


Figure S9. IR spectrum of 2,5-furandicarboxamide, FDC-subl and FDC-solv (attenuated total reflection, ATR).

S5 Mass spectra of the dicarboxamides

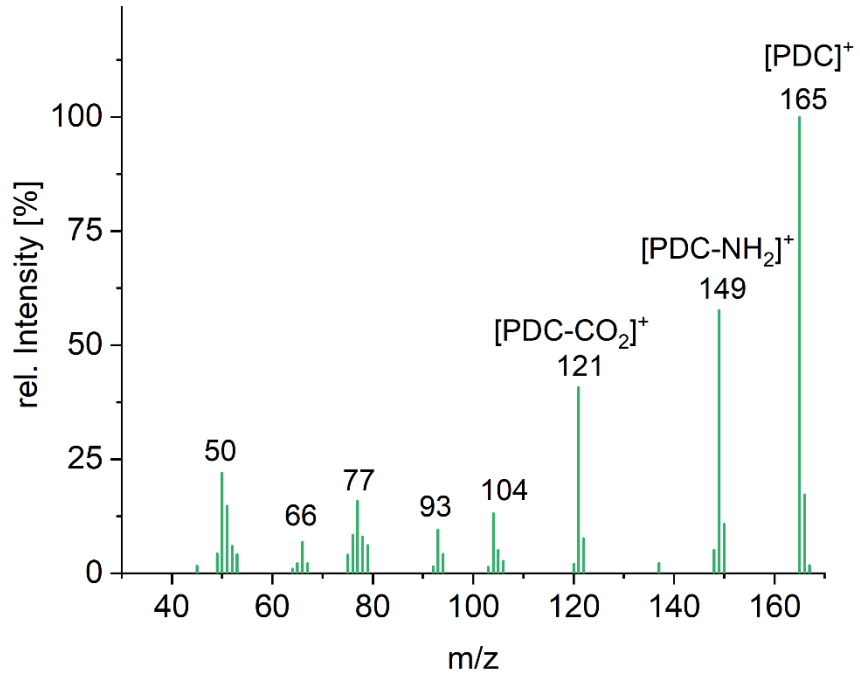


Figure S10. EI mass spectrum for 3,5-pyridinedicarboxamide, PDC.

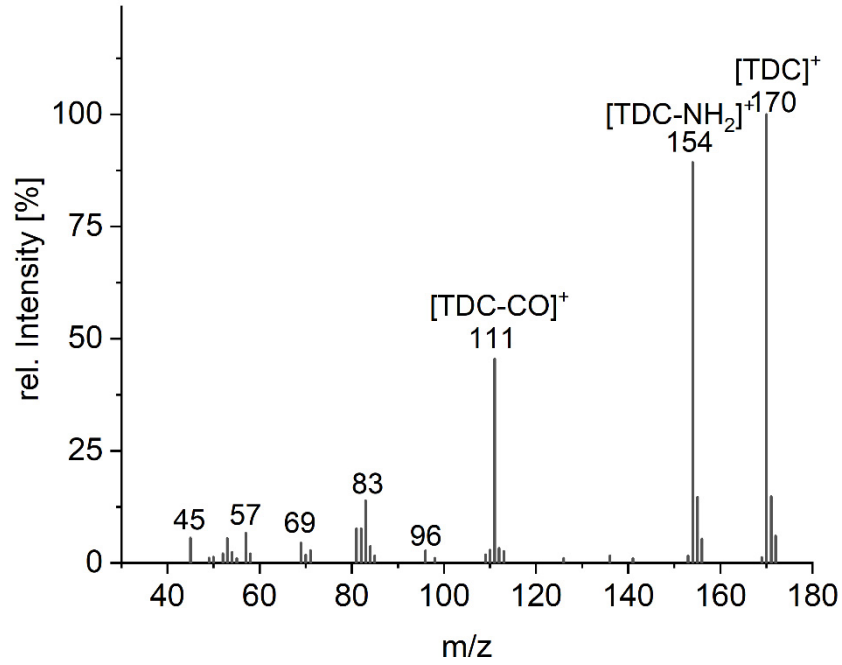


Figure S11. EI mass spectrum for 2,5-thiophenedicarboxamide, TDC.

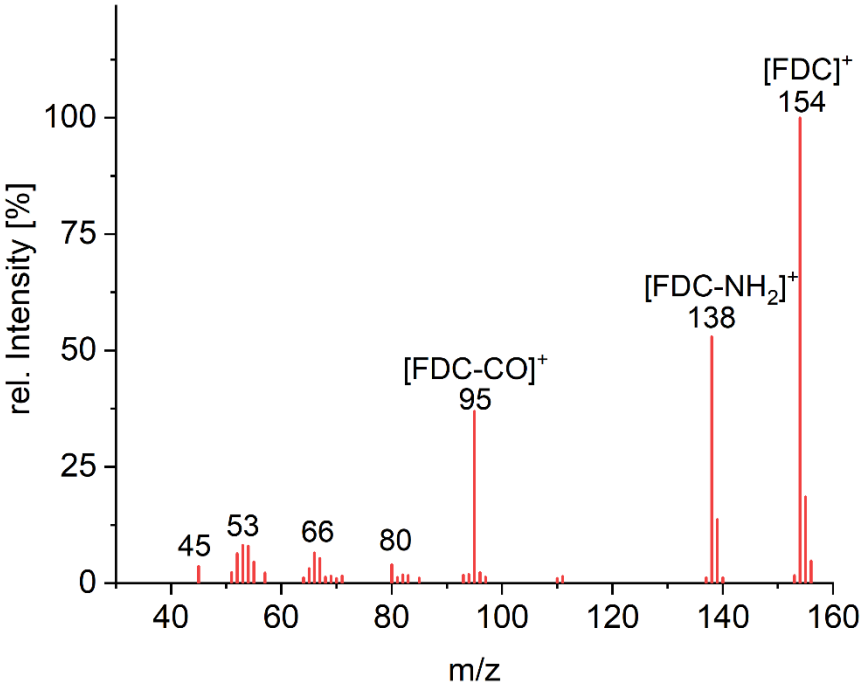


Figure S12. EI mass spectrum for 2,5-furandicarboxamide, FDC.

S6 PXRD spectra and Le Bail Fitting of the dicarboxamides

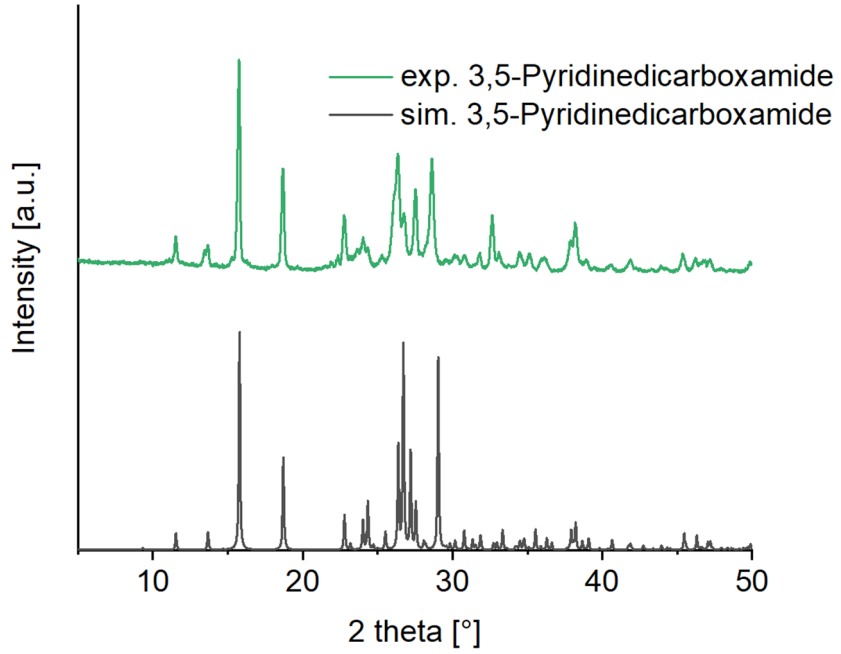


Figure S13. Simulated and experimental powder X-ray diffraction patterns of 3,5-pyridinedicarboxamide, PDC.

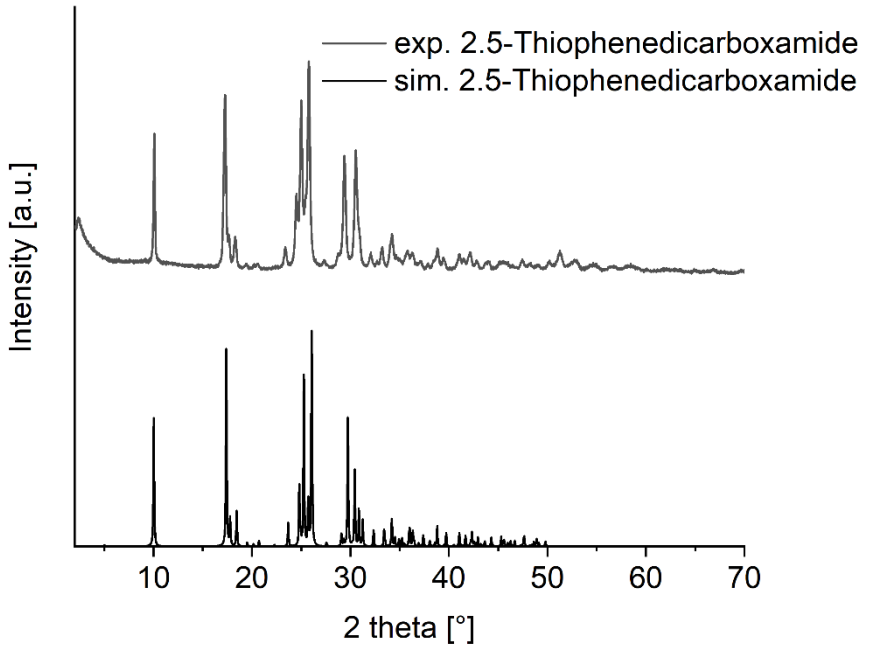


Figure S14. Simulated and experimental powder X-ray diffraction patterns of 2,5-thiophenedicarboxamide, TDC.

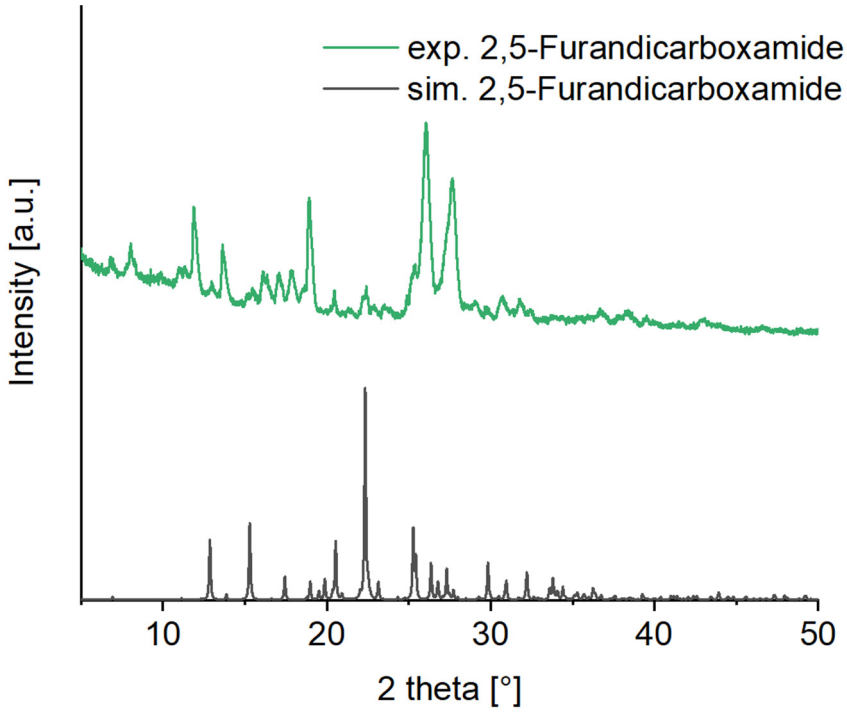


Figure S15. Simulated and experimental powder X-ray diffraction patterns of 2,5-furandicarboxamide for the FDC-subl structure.

To test the purity of the synthesized compounds, the PXRD data were fit using the Le Bail method (Jana 2006 software [2]). Unlike the Rietveld fit, the Le Bail fit, does not involve the information about the atom positions in the actual structure, but employs only cell level information (cell parameters, which are fittable, and the space group). A good Le Bail fit is a reliable indicator of purity. In the same time the Le Bail fit is, evidently, much less demanding regarding the data quality than the Rietveld fit, where the positions of the individual scatterers are taken into the account.

The PXRD data were collected by a Rigaku Miniflex PXRD diffractometer using Cu-K$\alpha_{1,2}$ radiation in a Bragg-Brentano geometry on a flat sample employing a low-background silicon sample-holder with an indent (for PDC and TDC) or a flat sample-holder (FDC, small amounts). The samples consisting of larger crystals were mildly ground (PDC and TDC), but no sieving or other further treatment was used.

The results show that the PDC is sufficiently pure, TDC contains some small amount of impurities (two small non-fitted peaks visible in the 2θ = 22-25° range), while the FDC contains the largest amount of impurities, but still not a critical amount (note the local deviations in the fit, including not very good peak shapes, which is, in part, due to low overall intensity of the measurement. Large scale sublimation yields a less pure product, so sublimation in a narrow tube was used, which allowed to reach higher purity. Worth noting, that the quality of the PXRD seemingly decreases with time, which is sign of slow hydration in air).

All in all, the compounds are sufficiently pure, at least for corroborating the viability of the synthetic method (with the exception of the relatively poor scalability of the FDC crystallization)

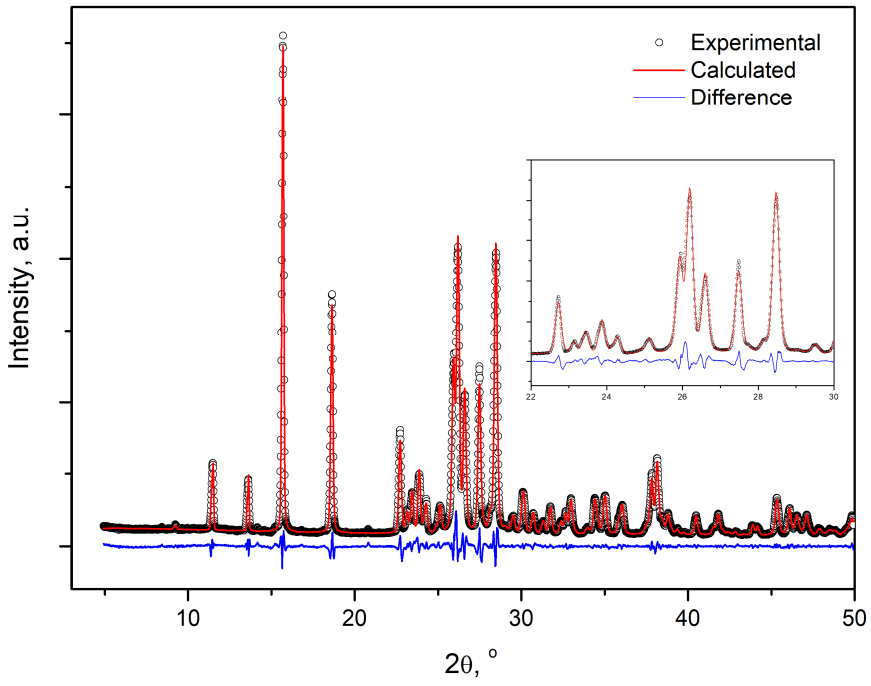


Figure S16 Le Bail fit of the PXRD data for PDC. The refined parameters for the room temperature measurement are a = 3.8674(3), b = 15.3658(12), c = 12.1857(12), and β = 96.023(4) in $P2_1/n$ (compare with the low temperature SCXRD with a = 3.78190(10), b = 15.3344(7), c = 12.1314(5), and β = 96.023(4)).

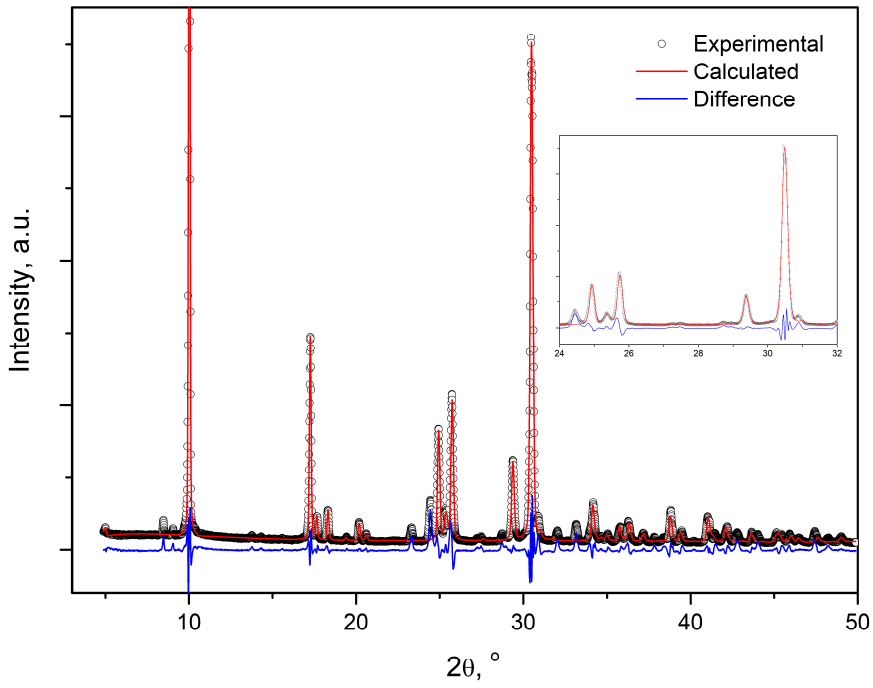


Figure S17 Le Bail fit of the PXRD data for TDC. The refined parameters for the room temperature measurement are a = 18.015(9), b = 3.8174(11), c = 10.286(4), β = 102.58(3) in $P2_1/c$ (compare with the low temperature SCXRD with a = 18.0336(5), b = 3.84290(10), c = 10.2084(3), β = 102.507(3)).

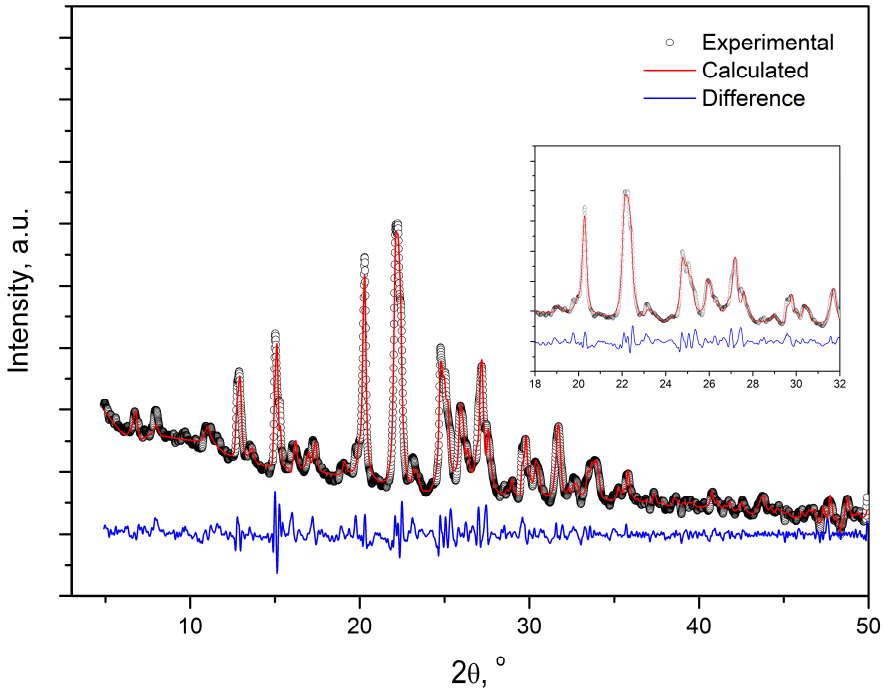


Figure S18 Le Bail fit of the PXRD data for FDC. The refined parameters for the room temperature measurement are a = 13.3617(13), b = 10.1446(12), c = 10.5255(12), β = 104.748(6) in $P2_1/c$ (compare with the low temperature SCXRD with a = 13.3086(3), b = 10.16340(10), c = 10.5981(2), β = 106.399(2)).

S7 2D Hirshfeld plots of the dicarboxamides

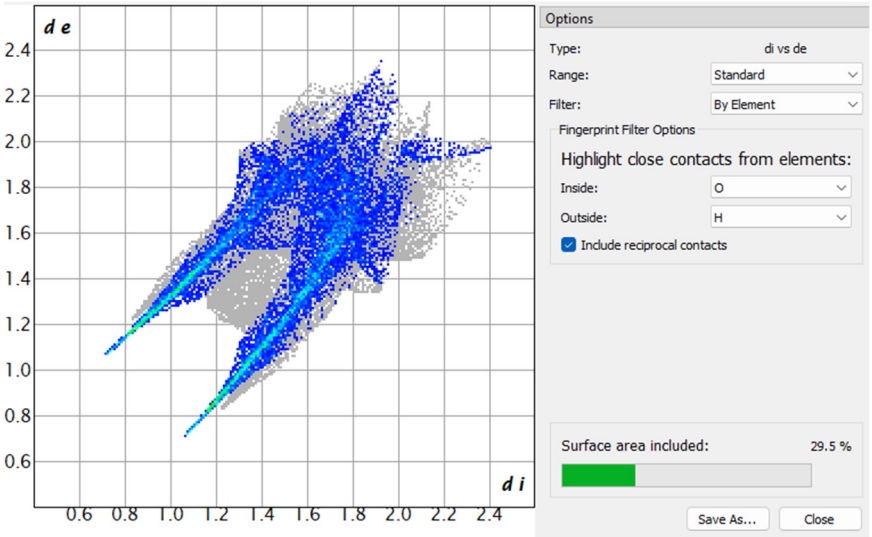


Figure S19. Contribution of O···H contacts in the Hirshfeld 2D plot of 3,5-pyridinedicarboxamide, PDC.

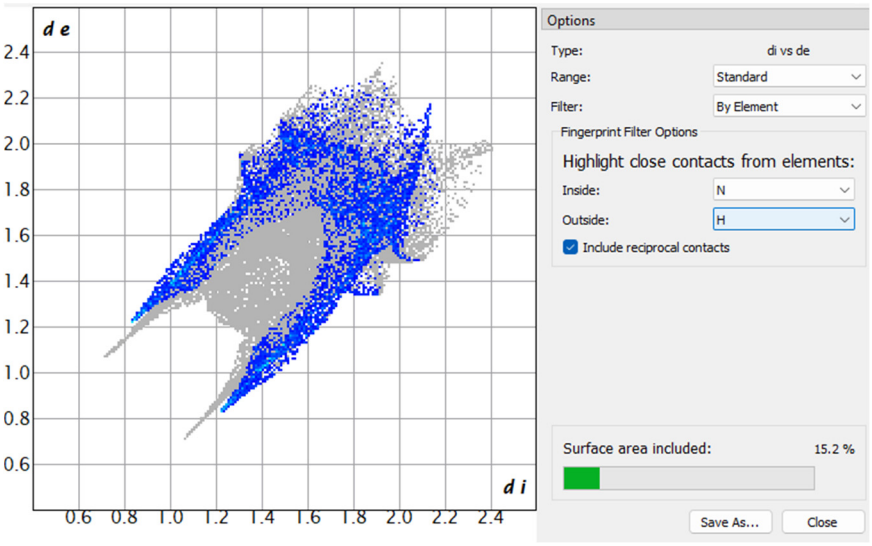


Figure S20. Contribution of N···H contacts in the Hirshfeld 2D plot of 3,5-pyridinedicarboxamide, PDC.

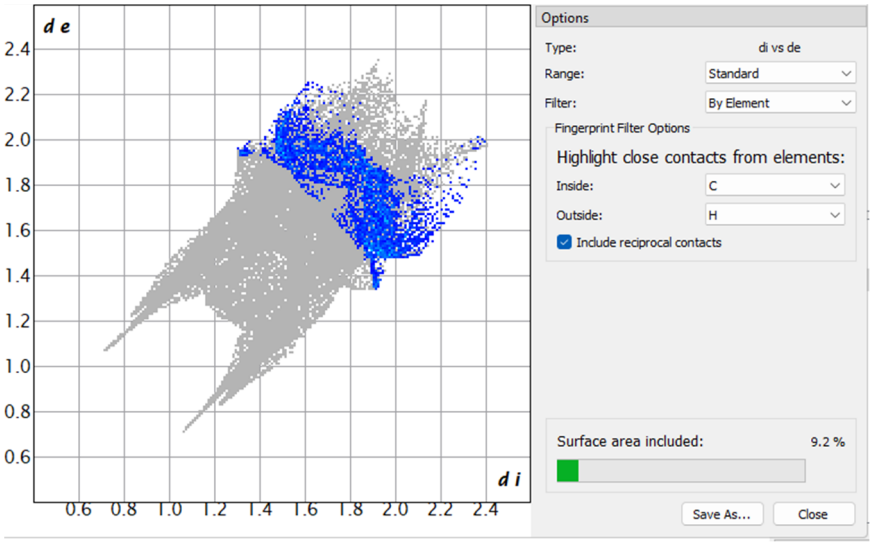


Figure S21. Contribution of C···H contacts in the Hirshfeld 2D plot of 3,5-pyridinedicarboxamide, PDC.

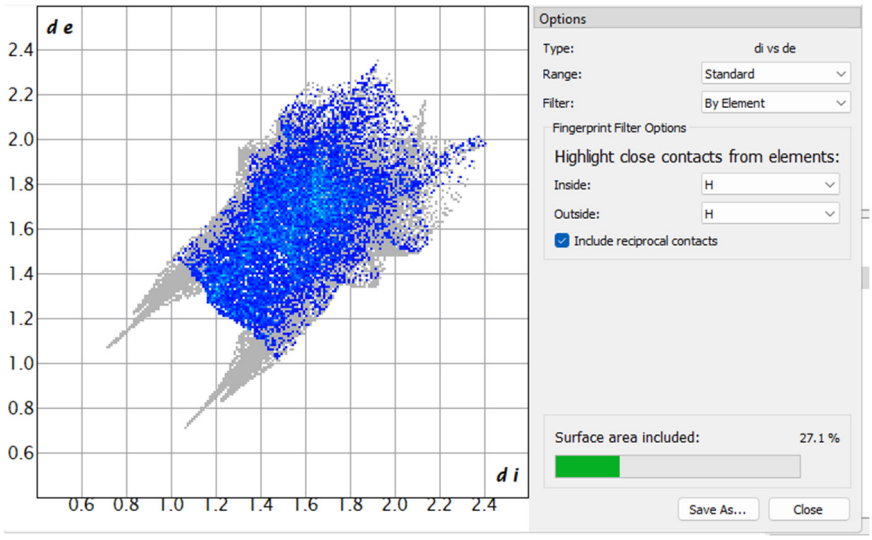


Figure S22. Contribution of H···H contacts in the Hirshfeld 2D plot of 3,5-pyridinedicarboxamide, PDC.

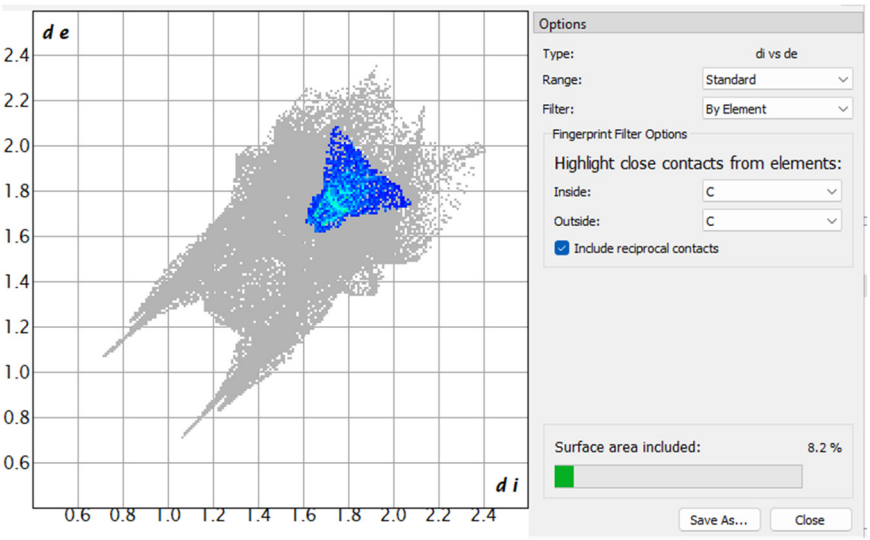


Figure S23. Contribution of C···C contacts in the Hirshfeld 2D plot of 3,5-pyridinedicarboxamide, PDC.

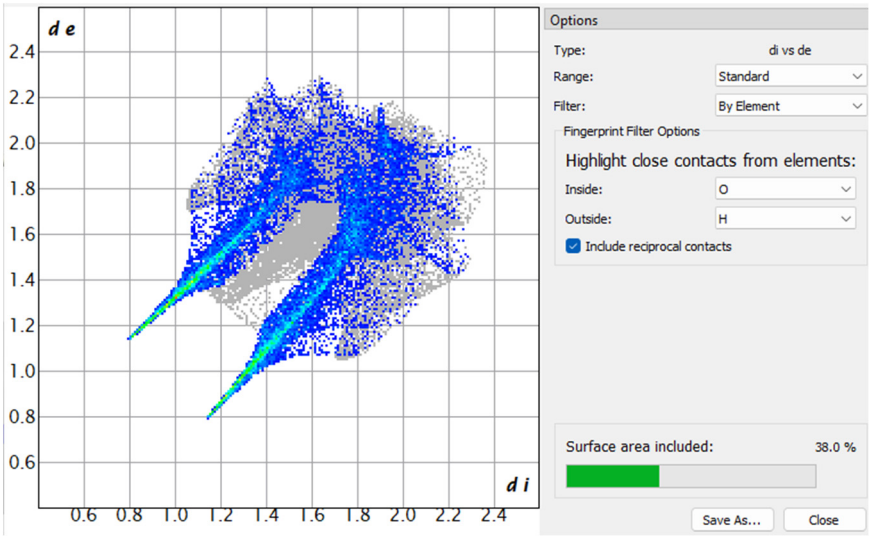


Figure S24. Contribution of O···H contacts in the Hirshfeld 2D plot of 2,5-thiophenedicarboxamide, TDC.

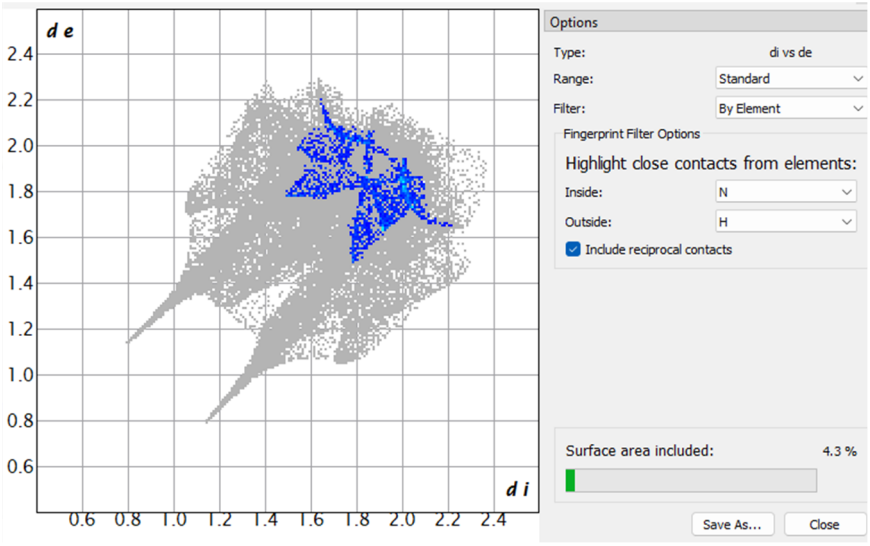


Figure S25. Contribution of N···H contacts in the Hirshfeld 2D plot of 2,5-thiophenedicarboxamide, TDC.

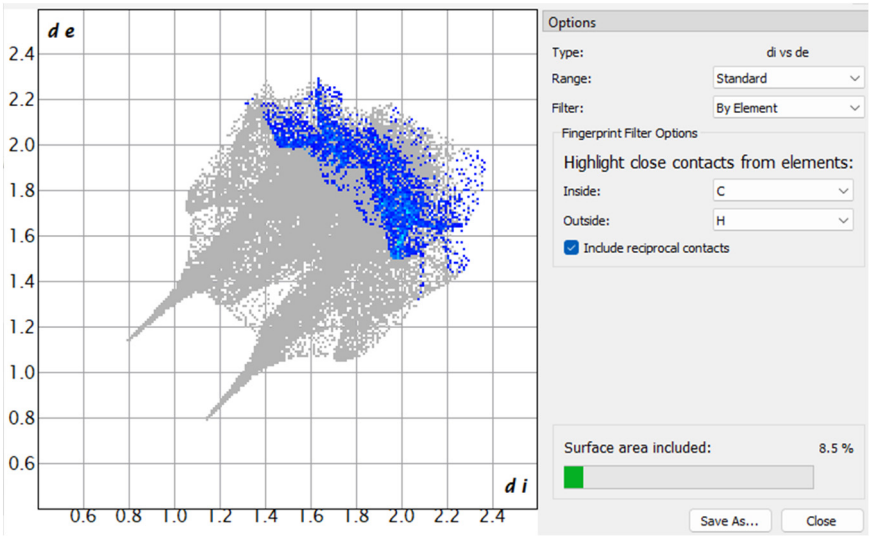


Figure S26. Contribution of C···H contacts in the Hirshfeld 2D plot of 2,5-thiophenedicarboxamide, TDC.

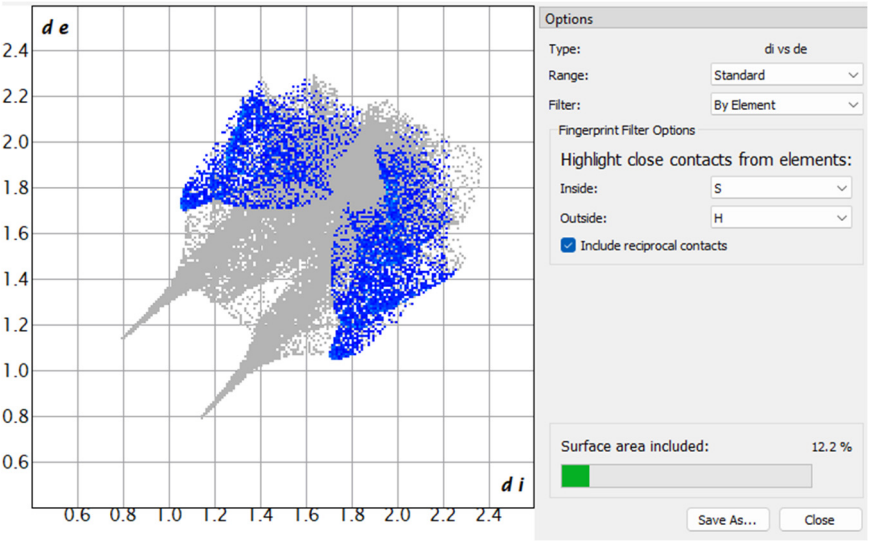


Figure S27. Contribution of S···H contacts in the Hirshfeld 2D plot of 2,5-thiophenedicarboxamide, TDC.

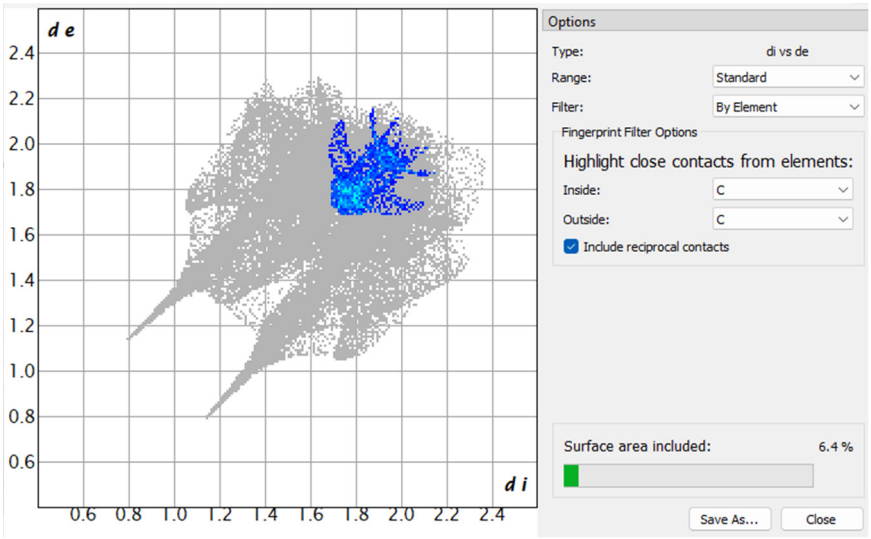


Figure S28. Contribution of C···C contacts in the Hirshfeld 2D plot of 2,5-thiophenedicarboxamide, TDC.

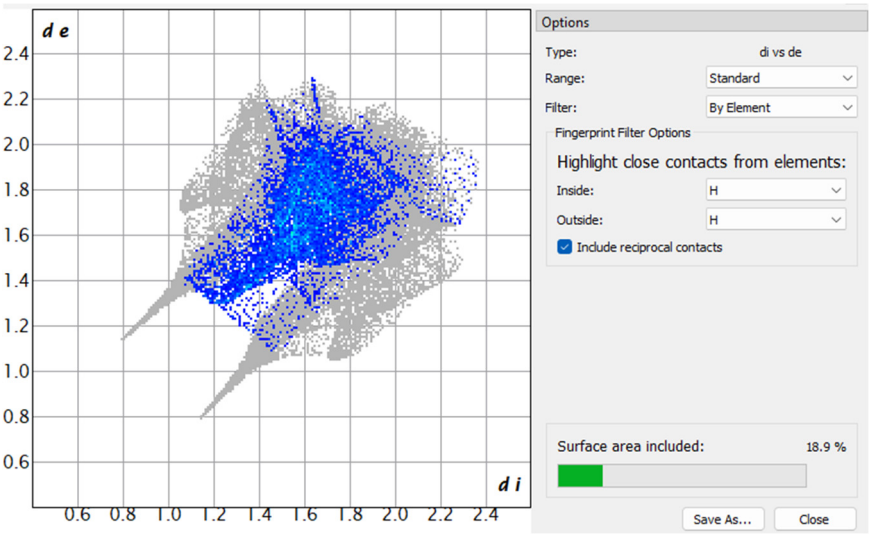


Figure S29. Contribution of H···H contacts in the Hirshfeld 2D plot of 2,5-thiophenedicarboxamide, TDC.

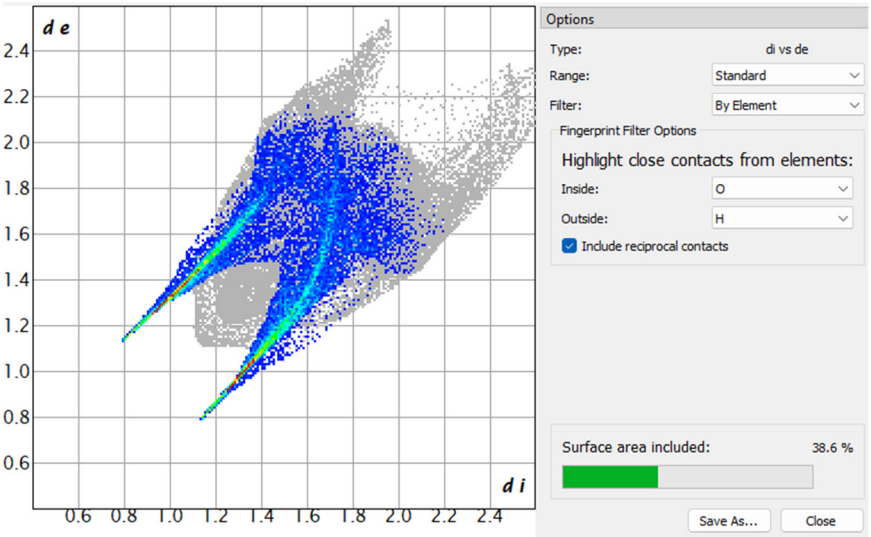


Figure S30. Contribution of O···H contacts in the Hirshfeld 2D plot of 2,5-furandicarboxamide for the FDC-solv structure.

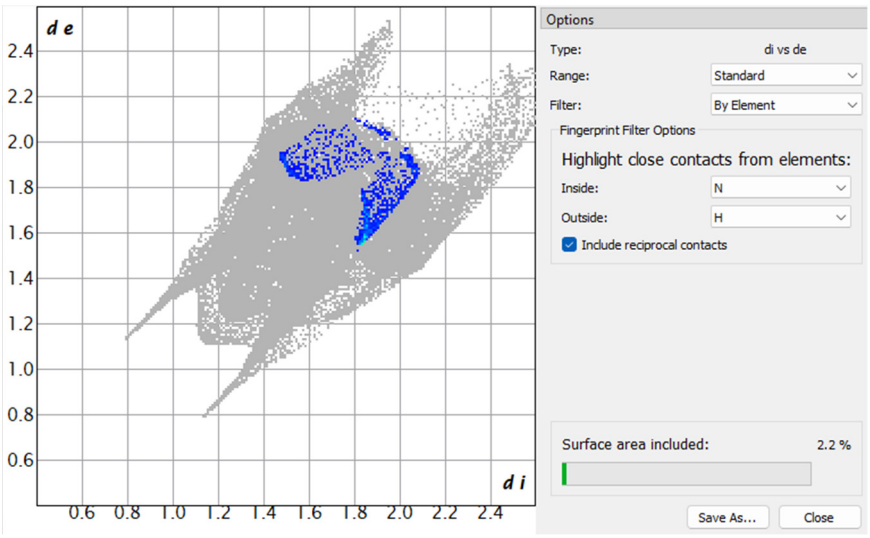


Figure S31. Contribution of N···H contacts in the Hirshfeld 2D plot of 2,5-furandicarboxamide for the FDC-solv structure.

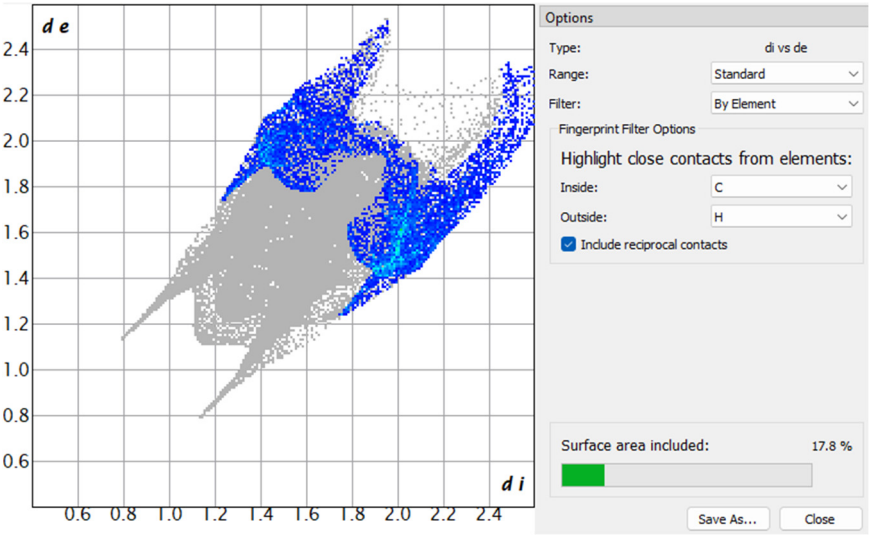


Figure S32. Contribution of C···H contacts in the Hirshfeld 2D plot of 2,5-furandicarboxamide for the FDC-solv structure.

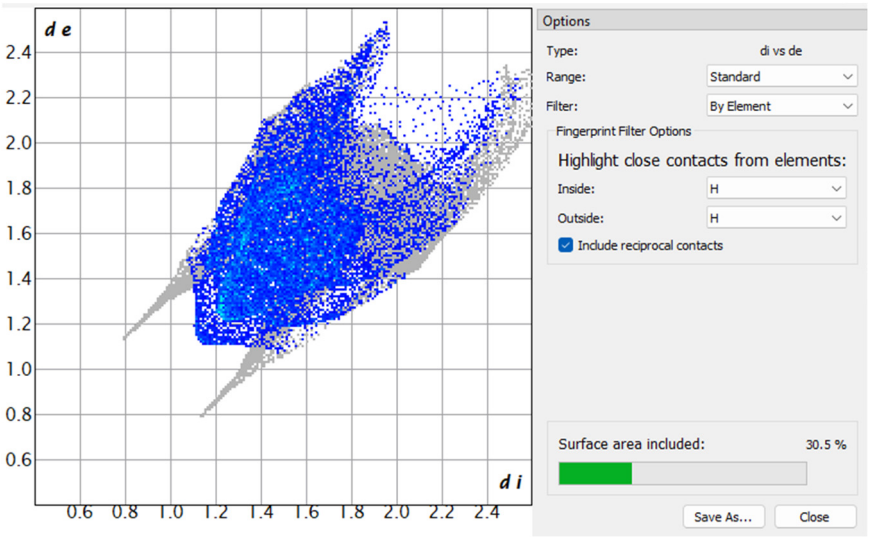


Figure S33. Contribution of H···H contacts in the Hirshfeld 2D plot of 2,5-furandicarboxamide for the FDC-solv structure.

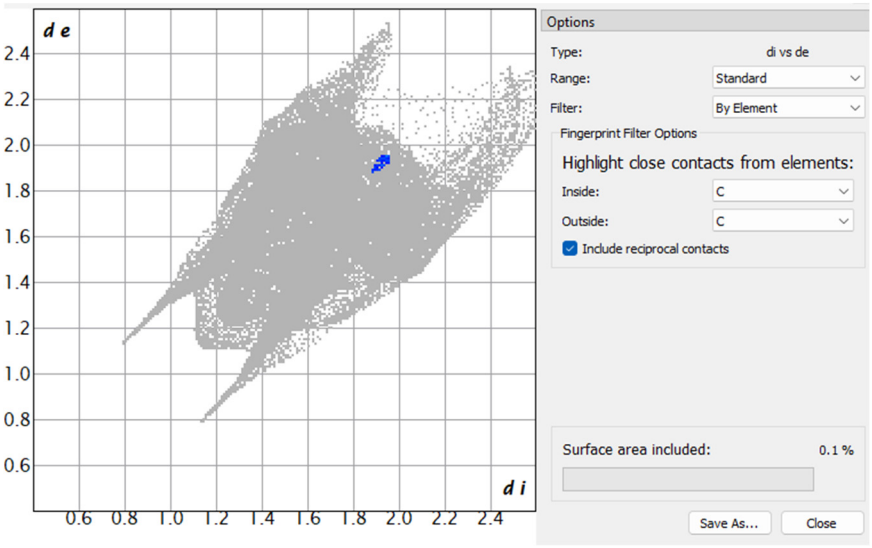


Figure S34. Contribution of C···C contacts in the Hirshfeld 2D plot of 2,5-furandicarboxamide for the FDC-solv structure.

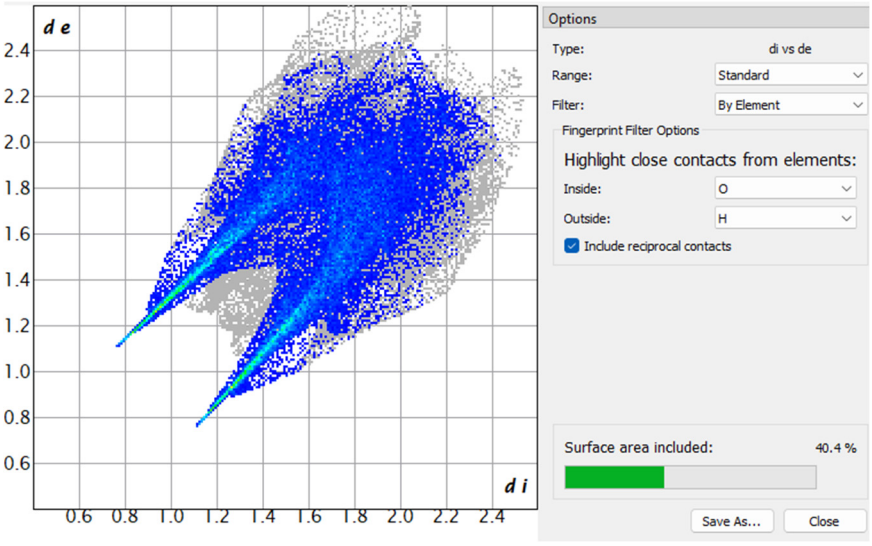


Figure S35. Contribution of O···H contacts in the Hirshfeld 2D plot of 2,5-furandicarboxamide for the FDC-subl structure.

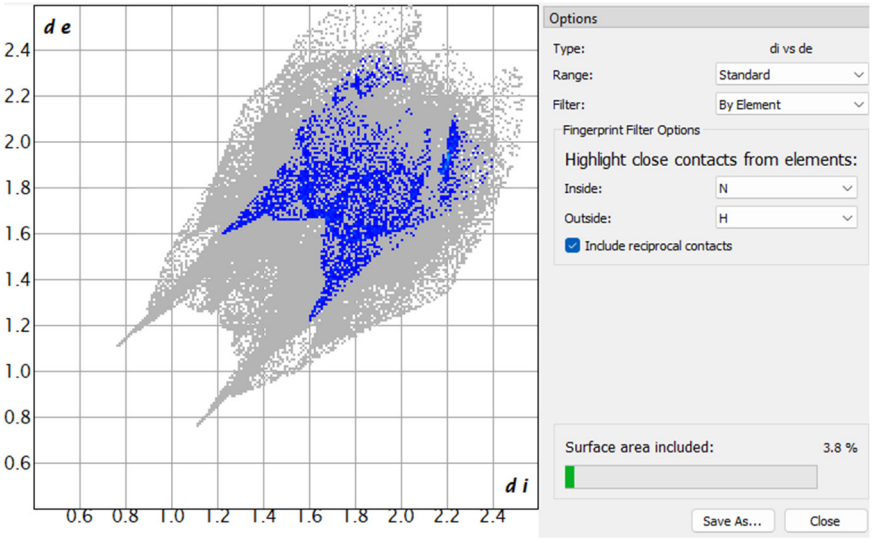


Figure S36. Contribution of N···H contacts in the Hirshfeld 2D plot of 2,5-furandicarboxamide for the FDC-subl structure.

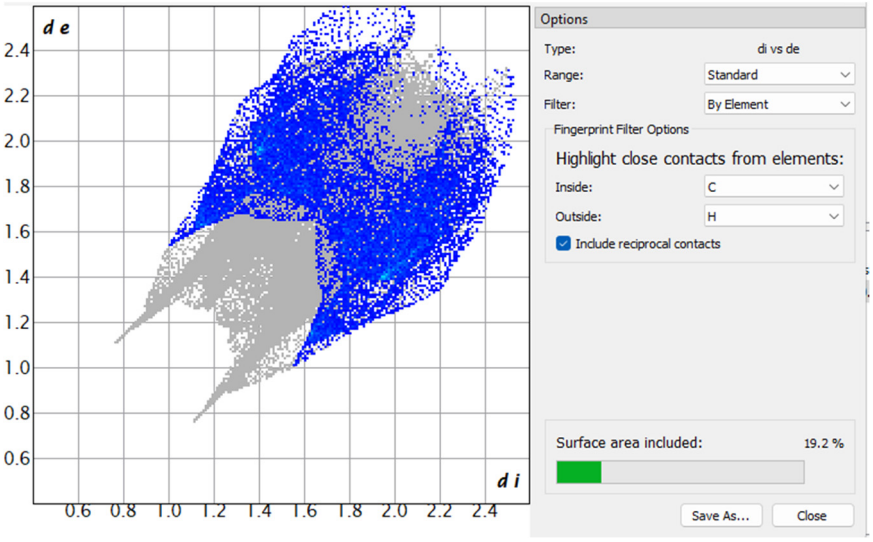


Figure S37. Contribution of C···H contacts in the Hirshfeld 2D plot of 2,5-furandicarboxamide for the FDC-subl structure.

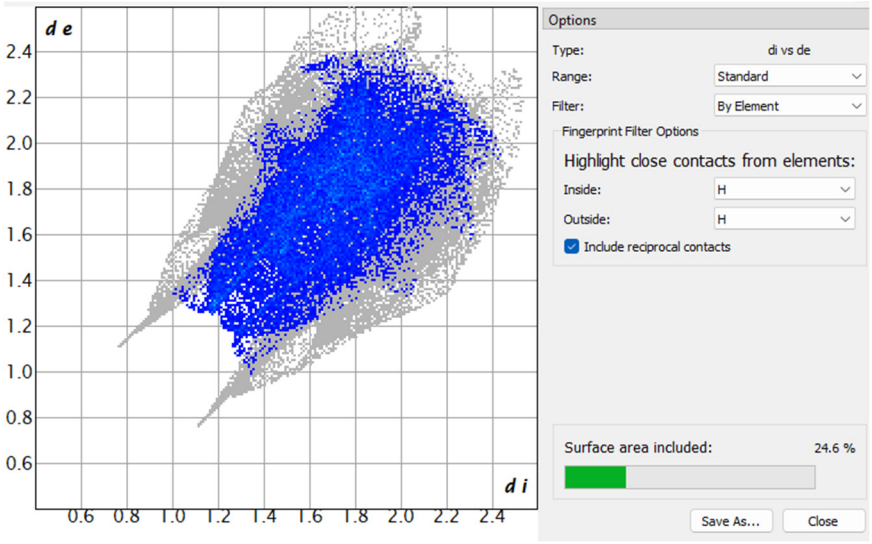


Figure S38. Contribution of H···H contacts in the Hirshfeld 2D plot of 2,5-furandicarboxamide for the FDC-subl structure.

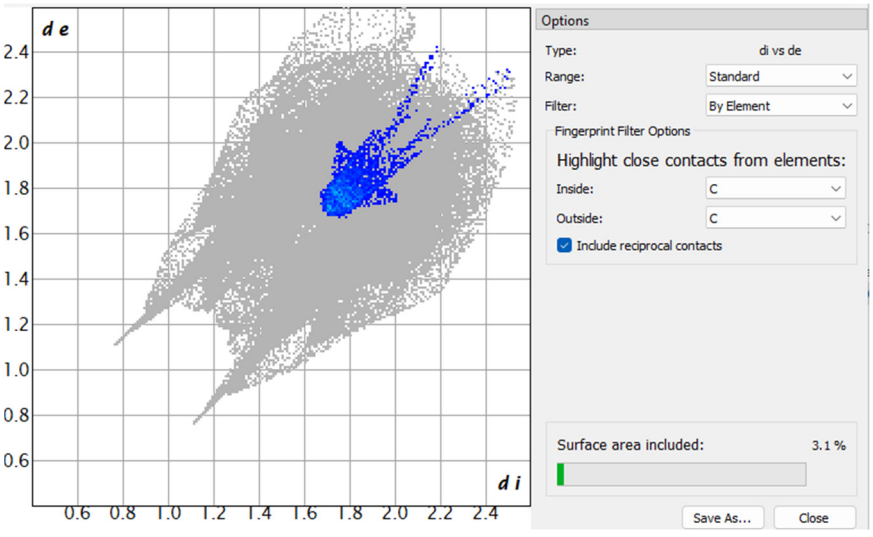


Figure S39. Contribution of C···C contacts in the Hirshfeld 2D plot of 2,5-furandicarboxamide for the FDC-subl structure.

References

1. Wu, Y.Y.; Meng, M.; Wang, G.Y.; Feng, P.; Liu, C.Y. Optically probing the localized to delocalized transition in Mo_2–Mo_2 mixed-valence systems. *Chem. Commun*. **2017**, *53*, 3030–3033**.** https://doi.org/10.1039/C7CC00119C
2. Petříček, V.; Dušek, M.; Palatinus, L. Crystallographic computing system JANA2006: general features. *Z. Kristallogr.-Cryst. Mater.* **2014**, *229*, 345–352. https://doi.org/10.1515/zkri-2014-1737